Real Time Quantification of Ultrafast Photoinduced Bimolecular Electron Transfer Rate: Direct Probing of the Transient Intermediate

ARTICLE *in* THE JOURNAL OF PHYSICAL CHEMISTRY B · JULY 2015

Impact Factor: 3.3 · DOI: 10.1021/acs.jpcb.5b03105 · Source: PubMed

3 AUTHORS, INCLUDING:

Puspal Mukherjee

Indian Institute of Technology Kanpur

6 PUBLICATIONS **9** CITATIONS

SEE PROFILE

Somnath Biswas

The Ohio State University

1 PUBLICATION **0** CITATIONS

SEE PROFILE

THE JOURNAL OF PHYSICAL CHEMISTRY B

Article

pubs.acs.org/JPCB

Real Time Quantification of Ultrafast Photoinduced Bimolecular Electron Transfer Rate: Direct Probing of the Transient Intermediate

Puspal Mukherjee, Somnath Biswas, and Pratik Sen*

Department of Chemistry, Indian Institute of Technology Kanpur, Kanpur 208 016, Uttar Pradesh, India

Supporting Information

ABSTRACT: Fluorescence quenching studies through steady-state and time-resolved measurements are inadequate to quantify the bimolecular electron transfer rate in bulk homogeneous solution due to constraints from diffusion. To nullify the effect of diffusion, direct evaluation of the rate of formation of a transient intermediate produced upon the electron transfer is essential. Methyl viologen, a well-known electron acceptor, produces a radical cation after accepting an electron, which has a characteristic strong and broad absorption band centered at 600 nm. Hence it is a good choice to evaluate the rate of photoinduced electron transfer reaction employing femtosecond broadband transient absorption spectroscopy. The time constant of the aforementioned process between pyrene and methyl viologen in methanol has been estimated to be 2.5 ± 0.4 ps using the same technique. The time constant for the backward reaction was found to be 14 ± 1 ps. These values did not change with variation of concentration of quencher, i.e., methyl viologen. Hence, we can infer that diffusion has no contribution in the estimation of rate constants. However, on changing the solvent from methanol to ethanol, the time constant of the electron transfer reaction has been found to increase and has accounted for the change in solvent reorganization energy.

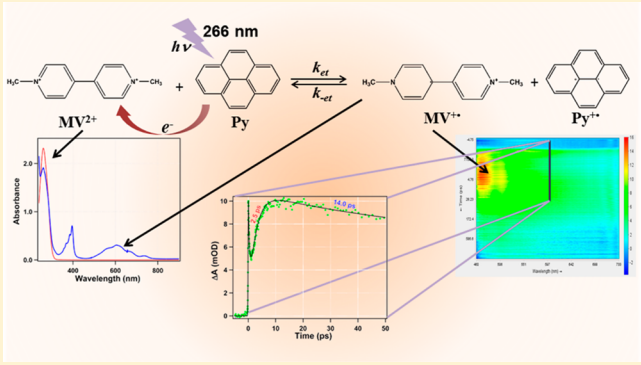

1. INTRODUCTION

Electron transfer (ET) reactions are omnipresent in nature. In many chemical and biological processes such as in photosynthesis and metabolism, ET reactions play a pivotal role.[1−12] A very important category of ET reactions is the photoinduced electron transfer (PET) reaction. PET has been used to concur some of the greatest challenges of human survival, like energy harvesting from sunlight and mimicking our sources for food.[13,14] As anticipated, during the 20th and 21st century there have been extensive studies in the literature on PET due to its potential to meet the energy demand of the universe.[15−17] The knowledge of PET reactions enables Thomas J. Meyer and his group to explore[18] the solar energy conversion process. Many have approached the problem using semiconductors, vesicles, and different molecular systems.[18,19] The introduction of dye sensitized solar cell[20] by Michael Grätzel completely revolutionized the field of light harvesting. PET chemistry allows exploiting the energy stored in the excited state to be utilized chemically. So, it is indispensable to investigate the ultrafast excited state dynamics of PET to model a PET system for numerous practical applications.

From the 19th century, researchers have tried to explain the kinetics of PET.[10] Succeeding a prolonged study and discussion, Rudolph A. Marcus[21−23] first introduced the theory of ET in 1956. He was the pioneer in successfully interpreting the relation between reaction exergonicity and activation energy of the reaction with the involvement of nuclear and solvent reorganization.[21−24] One of the supreme predictions[25] of his bimolecular ET theory was the possibility of "inverted" chemical behavior, which is universally known as "Marcus inversion", and a parabolic relationship between the rate constant for PET with reaction exergonicity was predicted as given in eq 1. The rate constant of bimolecular ET reaction (k_{et}) can be[26] written in terms of electronic coupling matrix element (V_{el}), reorganization energy (λ; where λ is the sum of intramolecular (λ_i) and solvent reorganization (λ_s) contribution), and the free energy change (ΔG°) of the ET reaction.

$$k_{et} = \frac{4\pi^2}{h}\frac{V_{el}^2}{\sqrt{4\pi\lambda_S k_B T}}\exp\left\{-\frac{(\Delta G^\circ + \lambda)^2}{4\lambda k_B T}\right\} \quad (1)$$

As long as $-\Delta G^\circ < \lambda$, k_{et} would increase with increasing the reaction exergonicity, which is the normal behavior. As the reaction exergonicity increase up to a certain point, where $-\Delta G^\circ = \lambda$, k_{et} attains its maximum value. This specific behavior is widely known as Marcus barrierless condition for ET reaction. If the exergonicity increases beyond λ, where $-\Delta G^\circ >$

Special Issue: Biman Bagchi Festschrift

Received: March 31, 2015
Revised: May 29, 2015
Published: July 1, 2015

DOI: 10.1021/acs.jpcb.5b03105
J. Phys. Chem. B 2015, 119, 11253−11261

Scheme 1. Kinetic Depiction of Bimolecular Photoinduced Electron Transfer Reaction

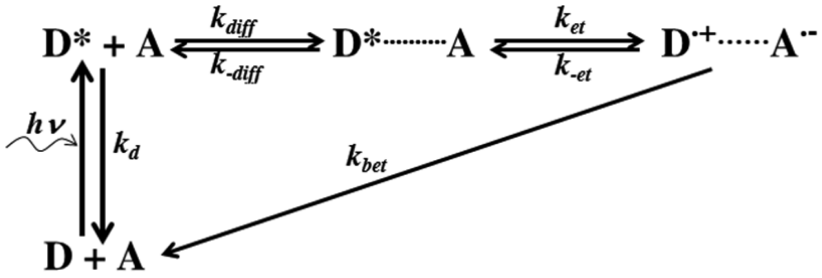

λ, k_{et} would gradually decrease as the reaction exergonicity goes up. This exergonic region is universally known as Marcus inverted region (MIR). Since then there have been several attempts[27−35] to prove this captivating theoretical prediction. However, major studies failed to establish the theory as in bulk solution the PET rate constant reaches the diffusion controlled limit at moderately exergonic condition and remains same at higher exergonicity too. Unavailability of electron donor−acceptor pair with such high exergonicity put the limit on observation of MIR in low viscosity solvents. The first successful experimental evidence[36] of the existence of MIR came from Miller and co-workers after almost 25 years of its prediction. They surmount the effect of diffusion by employing a constant distance between the donor and the acceptor and eventually that was the case of intramolecular PET.

The most routine method to study PET reaction is through fluorescence quenching.[37] Studies of the dynamic quenching process for an emissive donor or acceptor leads to the quenching rate constant (k_q) through the Stern−Volmer method. Thus, one can obtain an overall rate constant for the PET process. Using this method, people have studied the bimolecular PET reaction in neat solvent (intrinsic donor) media to obtain a detailed mechanistic and dynamical understanding, where the ET rate is faster than solvation and diffusion.[38−42] Many researchers have investigated the PET reaction in the confined environment as the solvent motion is retarded in the confined media like micelles, reverse micelles, cyclodextrins, etc., and the reorganization energy (λ) would be small.[26,43−55] A slower diffusion rate in the confined media also facilitates the situation. As a result, the bell-shaped dependence of k_q with the reaction exergonicity (MIR) could be observed at much lower reaction exergonicity.[43−55] Study of PET in highly viscous ionic liquids revealed a slower k_q value which has accounted for the extremely slow diffusion of reactants.[56,57]

Scheme 1 depicts the formation and fate of the encounter complex and the formation of radical ions during a bimolecular PET reaction. In Scheme 1, k_d is radiative rate of deactivation of donor, k_{diff} and k_{-diff} are the diffusional rate constants, k_{et} is the unimolecular rate of electron transfer, k_{-et} is the rate of reversible electron transfer, and k_{bet} incorporates all the possible phenomena by which the ion pair can return to ground state configurations. Through a steady-state approximation on the encounter complex and the radical ions with an assumption that the forward ET rate constant (k_{et}) is much greater than the backward ET rate constant (k_{-et}), one can get the following simple relationship (a detailed kinetic analysis of Scheme 1 has been provided in the Supporting Information).[10,37,42,58]

$$\frac{1}{k_q} = \frac{1}{k_{diff}} + \frac{1}{k_{et}} \qquad (2)$$

If the ET process is the rate-determining step ($k_{et} \ll k_{diff}$), then the measured quenching rate constant (k_q) would provide the value of k_{et}, but for the diffusion controlled reaction where the diffusion process is the rate-determining step ($k_{et} \gg k_{diff}$), k_q is unable to quantify k_{et}. In other words, for the diffusion limited bimolecular PET reaction, the indirect quantification of k_{et} (by measuring k_q, i.e., the steady-state or time-resolved quenching experiments) is impertinent. A prolonged controversy among researchers persists over the observation of MIR. In recent years it has been shown that analyzing the data with a quenching model accounting for both static and transient domain of the process can result in the disappearance of MIR.[59] It was speculated by Vauthey and co-workers that the observation of MIR in confined systems is apparent and is an effect of viscosity of the solvent and the lifetime of the probe molecule.[60,61] Therefore, it is necessary to measure the actual ET rate between a donor and an acceptor, which is free from the effect of diffusion, and can be used to settle the controversy raised by Vauthey and co-workers. Understandably, fluorescence quenching experiments cannot serve the purpose. A direct measurement of bimolecular ET rate is rare in the literature as the distinction or elimination of the role of diffusion is extremely difficult. Nevertheless, the effect of diffusion in the bimolecular PET reaction could be nullified if the rate of transient intermediate (i.e., the product of the ET reaction) could be probed directly.

In this present contribution, we have studied the bimolecular PET rate between pyrene (Py) and methyl viologen (MV^{2+}), where the former is the donor and the latter is the acceptor, in low viscosity solvents like methanol (MeOH) and ethanol (EtOH) to directly measure the rate of bimolecular PET reaction without any constraints from diffusion. MV^{2+} is a well-known electron acceptor used in several ET reactions, e.g., electron ejection from gold nanoparticle,[62] modified Zn porphyrin,[63] tris(2,2-bipyridine)ruthenium(II),[64] etc. Upon accepting an electron, MV^{2+} forms a radical cation ($MV^{\bullet+}$), and that could be detected directly by the transient absorption spectroscopy. The rate of formation of the $MV^{\bullet+}$ would be exactly equal to the ET rate (k_{et}) as this is the product of the ET reaction, and the kinetics of formation of $MV^{\bullet+}$ from the encounter complex is a first order and unimolecular process even if the overall kinetics is second order and bimolecular.[10,37,42,58] In this way, the contribution of the diffusion can be excluded fully from the calculated rate constant of bimolecular PET.

2. MATERIALS AND METHODS

Pyrene and methyl viologen (Scheme 2) were purchased from Sigma-Aldrich and used as received. For this study we have used high performance liquid chromatography grade methanol, which was obtained from Merck, India, and ethanol was

DOI: 10.1021/acs.jpcb.5b03105
J. Phys. Chem. B 2015, 119, 11253−11261

Scheme 2. Chemical Structure of (a) Pyrene (Donor) and (b) Methyl Viologen (Acceptor)

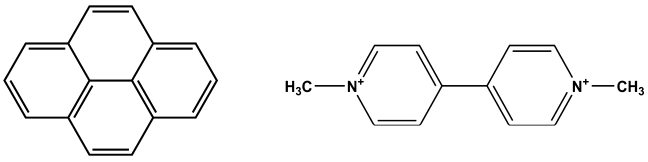

(a) (b)

purchased from Changshu Yangyuan Chemical, China. Both the solvents were distilled prior to use.

The UV−vis absorption spectra and fluorescence spectra were recorded using a commercial UV−vis spectrophotometer (V-670, JASCO, Japan) and a spectrofluorimeter (Fluorolog-3, Jobin Yvon), respectively. Fluorescence lifetime was measured by time correlated single photon counting (TCSPC) method using a commercial setup from Jobin-Yvon. For lifetime measurement, all the samples were excited using a pulsed nano-LED (340 nm, <1 ns, 1 MHz). The instrument response function was 1.4 ns. All the experiments were carried out at room temperature.

Cyclic voltammetric (CV) experiments were performed at 298 K by using CH instruments, Electrochemical Analyzer/Workstation model 600B series. The cell contains a Beckman M-39273 platinum-inlay working electrode, a Pt wire auxiliary electrode, and a saturated calomel electrode (SCE) as reference electrode. For coulometry, a platinum wire-gauze was used as the working electrode. The solutions were ∼1.0 mM sample and 0.1 M supporting electrolyte, tetrabutylammonium perchlorate or lithium chloride, as needed. Spectroelectrochemical measurements were performed using a custom-made cell (Model EF-1350) from Bioanalytical Systems Inc. The measured redox potentials at 298 K were converted to the ferrocenium/ferrocene (Fc^+/Fc) reference. Under our experimental conditions, the $E_{1/2}$ and peak-to-peak separation ΔE_p values (CH_2Cl_2) for couple Fc^+/Fc were 0.49 V and 120 mV versus SCE, respectively.[65]

All femtosecond transient absorption (TA) measurements were performed in a commercially available spectrometer (Femto-Frame-II, IB Photonics, Bulgaria). The laser system used for transient absorption experiments consisted of a mode-locked Ti:sapphire femtosecond oscillator (MaiTai SP, Spectra-Physics) and a Ti:sapphire regenerative amplifier (Spitfire Pro XP, Spectra-Physics) pumped by a 20-W Q-switched Nd:YLF laser (Empower, Spectra-Physics). The amplifier generated 80 fs pulses centered at 800 nm at a 1 kHz repetition rate with energy of ∼4 mJ per pulse. The fundamental beam was split into two beams by a beam splitter, and the major proportion was used to generate the pump pulse. Frequency doubling was performed in a 0.2 mm β-barium borate (BBO) crystal. The fundamental (800 nm) and the second harmonic beam (400 nm) were collected collinearly in another 0.2 mm BBO crystal to generate the third harmonic light (266 nm). A small portion of the fundamental light was allowed to pass through a computer-controlled motorized delay stage and was used to generate white-light continuum with a spectral range of 450−770 nm by focusing it on a 0.3 mm sapphire crystal. All measurements were performed with a pump energy of ca. 1 μJ, and the polarization of the pump was set at the magic angle (54.7°) with respect to the probe beam. The probe was delayed in time relative to the pump pulse using an optical delay line providing a maximum time window of 2.0 ns. The probe beam after transmission through a sample cell was focused onto a 200 μm optical fiber and was then dispersed by means of a polychromator onto a CCD camera. The overall instrument response function is 120 fs. The data obtained were fitted globally using GLOTARAN software.[66]

3. RESULTS AND DISCUSSION

3.1. Quenching Studies. Quenching of Py emission by MV^{2+} by means of bimolecular PET process has been studied using steady-state and time-resolved fluorescence spectroscopic measurements. As PET is a dynamic quenching process, one of the most familiar ways to study this is the Stern−Volmer method. MV^{2+} has an overlapping absorption spectrum with Py in MeOH (Figure S1 of Supporting Information), but MV^{2+} does not show any emission even in very high concentration when excited around 340 nm. Thus, the emission spectra remained free of any contribution from MV^{2+}, and quenching of Py could be measured without any hindrance. For the steady-state and time-resolved measurements the sample was excited at 340 nm. Py shows its characteristic emission spectra in methanol (Figure 1), and with the addition of MV^{2+} to the

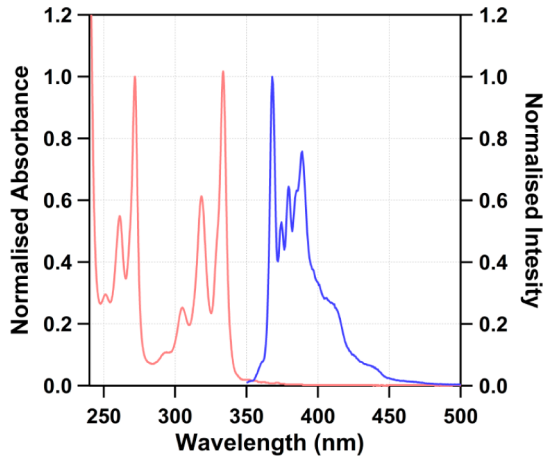

Figure 1. Absorption and emission spectra of pyrene in methanol.

solution of Py in MeOH, a monotonous decrease in the emission intensity and fluorescence lifetime was observed (see Figures S2 and S3 in the Supporting Information). To calculate the average lifetime of Py at each concentration of MV^{2+}, we have fitted the lifetime data using a sum of two exponentials. The time components and their amplitudes obtained from the fitting were used to calculate the average lifetime using the following equation:

$$\tau_{avg} = \frac{a_1\tau_1 + a_2\tau_2}{a_1 + a_2} \quad (3)$$

From both steady-state and time-resolved data we have plotted (I_0/I) and (τ_0/τ) as a function of methyl viologen concentration ($[Q]$), which follows the following equations.

$$\frac{I_0}{I} = 1 + K_{SV}[Q] \quad (4)$$

$$\frac{\tau_0}{\tau} = 1 + k_q\tau_0[Q] \quad (5)$$

Here I_0 is the emission intensity of Py in absence of quencher (MV^{2+}), I is the emission intensity of Py in the presence of the

DOI: 10.1021/acs.jpcb.5b03105
J. Phys. Chem. B 2015, 119, 11253−11261

quencher (MV^{2+}), τ_0 is the fluorescence lifetime of Py in absence of quencher (MV^{2+}), and τ is the fluorescence lifetime of Py in the presence of quencher (MV^{2+}). For the entire range of concentration of the quencher used, the values of (I_0/I) and (τ_0/τ) did not deviate (Figure 2) from the linearity confirming

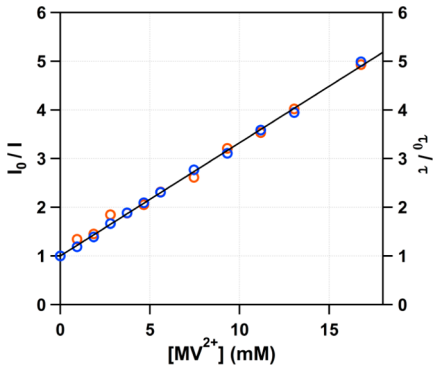

Figure 2. Stern–Volmer plot for quenching of pyrene by methyl viologen in methanol.

the existence of only one type of quenching process, i.e., dynamic quenching. From the slope of the linear plot the K_{SV} value is found to be 232 M^{-1}. The fluorescence lifetime of Py in MeOH in absence of quencher was measured to be 15.4 ns. Using this lifetime value, the k_q value is estimated to be 1.5×10^{10} M^{-1} s^{-1}. The k_q value thus obtained accounts for the electron transfer as well as diffusion of the reactants in MeOH. It is actually an overall combination of all the kinetic processes contributing to electron transfer process. For a chemical reaction the slower step is the rate-determining step. If the rate of diffusion is slower than the electron transfer, then k_q would be dominated by diffusion. Typically, the diffusion rate constant in a low viscosity solvent like MeOH is in the order of 10^{11} s^{-1}. In a comparison with k_q we can say that it is hard to estimate the rate of electron transfer as stated previously. That is the reason we turned our vision to a more direct approach of measuring the exact rate of electron transfer, i.e., through femtosecond TA spectroscopy.

3.2. Cyclic Voltammetry and Spectroelectrochemistry of MV^{2+}. To determine the reduction potentials of MV^{2+} we have performed the cyclic voltammetry measurement in MeOH. The first and second reduction potentials of MV^{2+} were found to be −0.43 and −0.90 V, respectively, as shown in Figure 3a, which is in agreement with the previously reported value.[64] It is evident that the first one corresponds to the formation of $MV^{\bullet+}$ (Scheme 3). Nevertheless, we have

Scheme 3. Reduction of Methyl Viologen (MV^{2+})

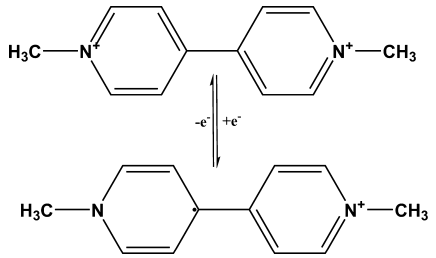

recorded the absorbance before the electrolysis and also after the first reduction of MV^{2+} to ensure the formation of the $MV^{\bullet+}$ by applying two different electrode potentials. MV^{2+} has an absorption peak around 260 nm in MeOH. The peak at 260 nm did not shift when −0.23 V which is less than the first reduction potential of MV^{2+} was applied (Figure 3b). However, at a greater potential, i.e., −0.63 V, a broad absorption band having a maximum around 605 nm appeared along with another peak at 396 nm. These two peaks were distinct characteristics of the $MV^{\bullet+}$ (Figure 3b).[67] The molar extinction coefficients of $MV^{\bullet+}$ reported in the previous study were 13 800 M^{-1} cm^{-1} (609 nm) and 42 700 M^{-1} cm^{-1} (396 nm).[67] As our broad band white light continuum in the TA setup perfectly overlaps with the 605 nm peak, we proceed to detect the rate of formation of $MV^{\bullet+}$ in real time.

3.3. Femtosecond TA Measurements. We have recorded the TA spectrum of Py in MeOH to compare it with the changes that occur upon addition of MV^{2+} to it. The excited state dynamics of Py is well-known and has been characterized by many spectroscopic methods including TA technique.[68,69] The molecule is said to undergo a very fast internal conversion (IC) from S_n to S_1 state followed by a vibrational cooling of the S_1 state on exciting at 266 nm.[68] As Py has a very long fluorescence lifetime in MeOH, it is understandable that we cannot observe the complete deactivation of the S_1 state of Py with our present experimental setup. However, we observed the early time dynamics as depicted in Figure 4 and compared it with the previously observed values. Essentially we have obtained three time constants for Py in MeOH, which are tabulated in Table 1. The pump beam (266 nm) excites Py

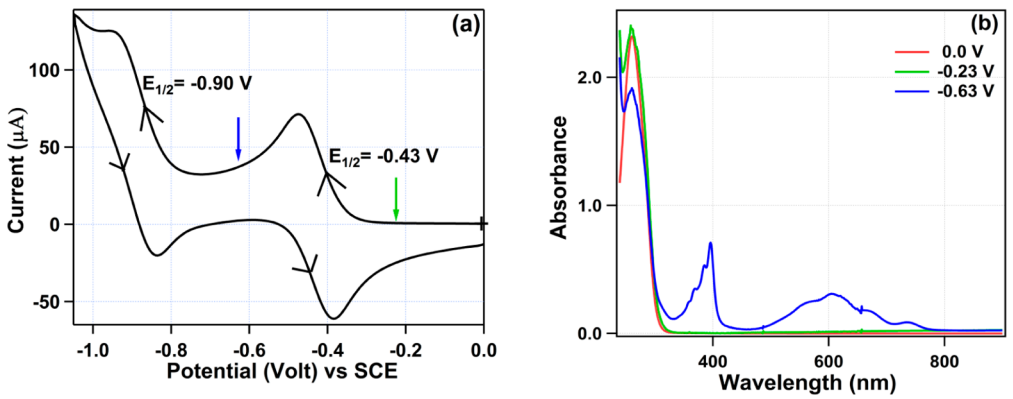

Figure 3. (a) Cyclic voltammetry of MV^{2+} in methanol and (b) absorption spectra of MV^{2+} at different electrode potentials (the arrows indicate the potential at which spectra were taken).

DOI: 10.1021/acs.jpcb.5b03105
J. Phys. Chem. B 2015, 119, 11253–11261

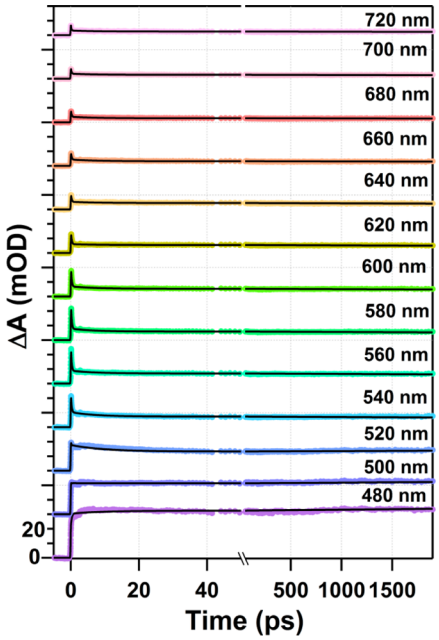

Figure 4. Plot of kinetic traces at different wavelength of Py in MeOH obtained from TA measurement (the black lines are the fitting results).

molecules to S_6 or higher state. The first time constant of 200 fs in MeOH has been attributed to the IC of S_6–S_1 state, and consequently, a vibrationally hot S_1 state is generated. In the next few picoseconds, the internal vibration relaxation occurred, and we obtained a time constant of ~7 ps. These values are in good agreement with the previously reported one.[68,69] The third long time component of 20 000 ps remains fixed during the fitting of the data, which corresponds to the lifetime of S_1 state and has no relevance in the present discussion. All the peaks in the transient absorption spectrum of Py have also been assigned. In the time domain of the first few picoseconds we have observed changes in the spectrum; however, beyond 60 ps no further change in the spectrum was observed. Following Miyasaka et al.[68] the absorption band around 470 and 510 nm in the TA spectrum of Py has been assigned to its excited state absorption S_1–S_{11} and S_1–S_{10}, respectively. The chances of excimer formation have been discarded due to the low concentration used in our study and the choice of our solvent being MeOH.

From cyclic voltammetry and spectroelectrochemistry measurements it is clear that $MV^{\bullet+}$ has a strong and broad absorption centered around 600 nm. The spectrum of our probe light spread over 460–750 nm gave us a perfect measurement condition to track the formation of $MV^{\bullet+}$ species. The bimolecular PET reaction between Py and MV^{2+} was probed directly by monitoring the formation of the $MV^{\bullet+}$ during the course of the reaction using transient absorption spectroscopic technique for the direct measurement of the rate of this bimolecular PET reaction. A mixture of Py (200 μM) and MV^{2+} (different concentration ca. 10, 20, 30, 40 mM) was used for this measurement and were excited at 266 nm. Figure 5a depicts the kinetics, and Figure 5b depicts the spectra obtained from Py–20 mM MV^{2+} in MeOH. The presence of a distinct rise component and its subsequent decay in the kinetic data around 600 nm region (absorption region of $MV^{\bullet+}$) signified the formation of $MV^{\bullet+}$ species by electron transfer from Py to MV^{2+} and subsequent back electron transfer process. This feature was absent in the kinetics of Py as discussed above, as well as in case of pure methyl viologen. This is to note that MV^{2+} also gets excited by 266 nm pump pulse; however, its excited state dynamics in 460–720 nm region does not reflect the formation of any new state (i.e., no rise time has been observed as can be seen in Figure S4 of the Supporting Information), which has also been reported earlier.[70] A comparison between the kinetics of Py, MV^{2+}, and a mixture of Py and 20 mM MV^{2+} at 600 nm (Figure S5 of the Supporting Information) clearly shows the existence of the growth in transient only for the last case. Thus, the assignment of the rise component observed in the Py–MV^{2+} mixtures to the electron transfer process is further supported. It is worth mentioning that the growth part did not start immediately after the excitation. The small time delay in the start of the growth part indicates that the reactants need a finite time to diffuse before the electron transfer could take place in the encounter complex. The decay part immediately after the growth component assigned to the back electron transfer process manifests that the species is indeed transient. The kinetic data were successfully fitted using a global fitting procedure using a sum of five exponential functions. The time constants are listed in Table 1. The τ_2, which is the rise time component, is found to be 2.5 ± 0.4 ps. The corresponding decay time (τ_3) is 14 ± 1 ps. The inverse of the τ_2 provide us the rate of electron transfer reaction between Py and MV^{2+}, which is 4×10^{11} s^{-1}. It is clear that this process is faster than the diffusion process. As diffusion has no role to play in the formation of $MV^{\bullet+}$ species in the encounter complex (which has been observed through TA measurement), the rate constant obtained is purely due to electron transfer. τ_4 and τ_5 are due to excited state dynamics of unreacted Py and MV^{2+}, and it is not straightforward to isolate and comment on them.

In the global fitting procedure, all the kinetics at different wavelengths were fitted using the same time constant, and account for the changes obtained in every wavelength. To prove this we have performed the transient absorption measurement with definite Py concentration and different

Table 1. Kinetic Rate Constants Obtained from Global Fitting

	solvent	τ_1[a] (ps)	τ_2[b] (ps)	τ_3[c] (ps)	τ_4[d] (ps)	τ_5 (ps)
Py	MeOH	0.2(d)	7.0(d)			20 000 (fixed) (d)
MV^{2+}	MeOH	0.4(d)	32.8(d)			8200(d)
Py (200 μM) + MV^{2+} (10 mM)	MeOH	0.5(d)	2.5(r)	13.5(d)	80(d)	5000(d)
Py (200 μM) + MV^{2+} (20 mM)	MeOH	0.6(d)	2.5(r)	14.0(d)	120(d)	4300(d)
Py (200 μM) + MV^{2+} (30 mM)	MeOH	0.5(d)	2.5(r)	14.0(d)	140(d)	4300(d)
Py (200 μM) + MV^{2+} (40 mM)	MeOH	0.6(d)	2.2(r)	14.0(d)	190(d)	4400(d)
Py (200 μM) + MV^{2+} (20 mM)	EtOH	0.5(d)	5.0(r)	15.0(d)	160(d)	4400(d)

[a] ±0.1 ps. [b] ±0.4 ps. [c] ±1 ps. [d] ±5 ps.

DOI: 10.1021/acs.jpcb.5b03105
J. Phys. Chem. B 2015, 119, 11253–11261

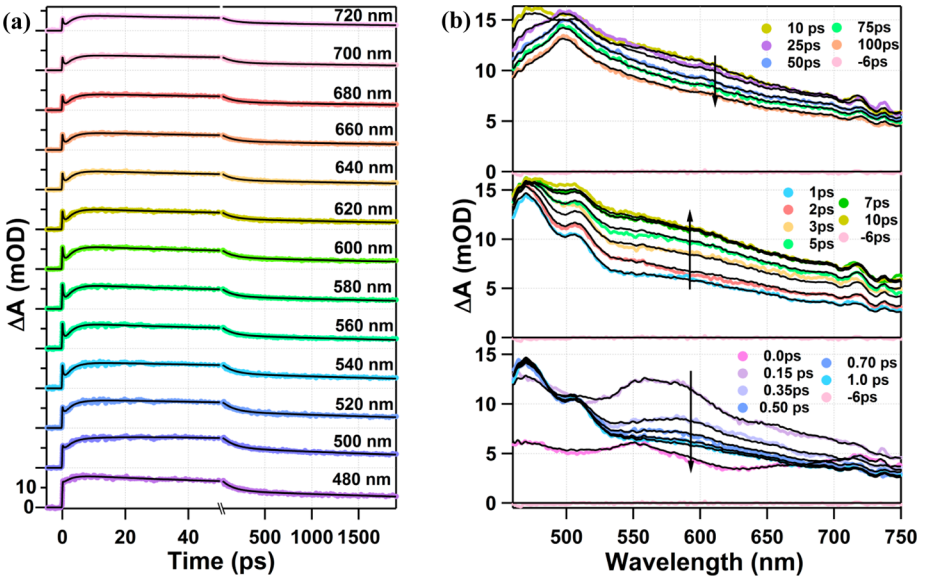

Figure 5. Plot of (a) kinetic traces at different wavelength and (b) spectra at different times of Py + 20 mM MV^{2+} in MeOH (the black lines indicate the fitting).

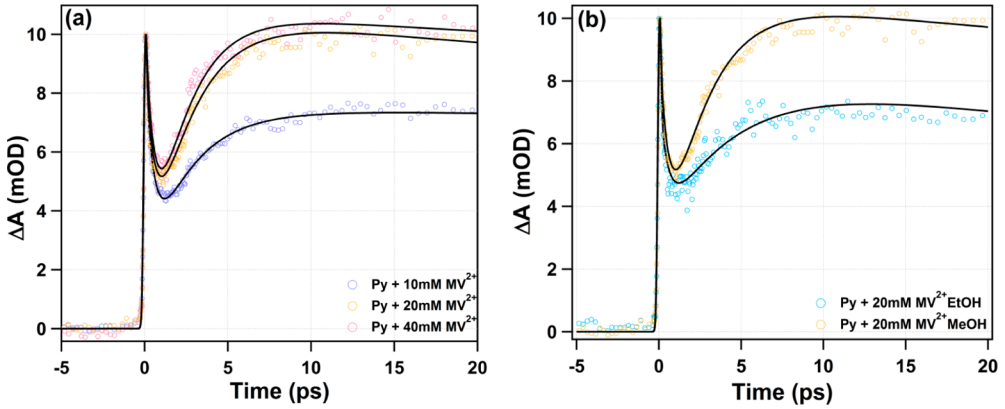

Figure 6. Plot of kinetic traces at 600 nm: (a) Py + different concentration of MV^{2+} in MeOH and (b) Py + 20 mM MV^{2+} in different solvents (the black lines indicate the fitting).

MV^{2+} concentration, i.e., 10, 20, 30 and 40 mM. The plots of kinetic data are shown in Figure S6 of the Supporting Information, Figure 5, and Figures S8 and S9 of the Supporting Information, respectively. A comparison of the effect of MV^{2+} concentration is also shown in Figure 6a. It clearly showed a similar kind of transient for all the different concentrations and was fitted by the same method. The time constants obtained for all the different concentrations of MV^{2+} are listed in Table 1. We can immediately see that neither the τ_2 nor the τ_3 varies with the concentration. As the variation of the concentration did not alter the process, we could confirm that it is purely due to forward and backward electron transfer between Py and MV^{2+}. Thus, we can conclude that, for the given donor−acceptor pair (Py and MV^{2+}), the rate constant for electron transfer is 4×10^{11} s^{-1}, and the same for back electron transfer is 7×10^{11} s^{-1} in MeOH.

3.4. Comparison of Rate of Bimolecular PET betwen Py and MV^{2+} in MeOH and EtOH. In the case of PET, k_{et} depends on solvent reorganization energy as evident from eq 1. Thus, if we change the medium, the rate of electron transfer is bound to change. To explore this we have studied the PET between the same pair (200 μM Py and 20 mM MV^{2+}) in EtOH (Figure S7 of Supporting Information). The presence of the rise and decay feature again signifies the effective electron transfer reaction. The time components obtained from the global fitting of the data have also been listed in Table 1. The time constant for forward electron transfer obtained is 5±0.4 ps, and the same for the back electron transfer, is 15±1 ps. The increase in the rise time component in ethanol compared to methanol (see Figure 6b) could be rationalized by higher solvent reorganization energy in ethanol. However, the backward electron transfer rate is almost similar in both cases.

4. CONCLUSION

PET reaction between Py and MV^{2+} has been monitored in low viscosity solvent by using femtosecond transient absorption measurement and has been compared with the conventional steady-state quenching data. The measured time component of the bimolecular PET reaction between Py and MV^{2+} in MeOH is 2.5 ± 0.5 ps. The forward as well as the backward ET rate did not vary with respect to the change in the acceptor concentration. As expected, the time component of the back ET rate (14 ± 1 ps) is higher than the forward one (2.5 ± 0.5 ps). The estimated values of k_{et} and k_q are, respectively, 4 ×

DOI: 10.1021/acs.jpcb.5b03105
J. Phys. Chem. B 2015, 119, 11253−11261

10^{11} s^{-1} and 1.5×10^{10} M^{-1} s^{-1}. The rate of electron transfer remains unchanged on increasing the concentration of the acceptor; however, a slower rate of electron transfer (2.5×10^{11} s^{-1}) was observed on changing the solvent from MeOH to EtOH. The higher reorganization energy in EtOH is attributed for this lower ET rate constant.

Likewise, this study, if we directly measure the bimolecular PET rate constant of several donor−acceptor pairs with varying exergonicity, the bell-shaped dependence of k_{et} with the reaction exergonicity in bulk homogeneous medium and in confined systems could be ascertained.

■ ASSOCIATED CONTENT

Supporting Information

Kinetic analysis of the bimolecular electron transfer scheme, absorption spectra of Py and MV^{2+} in MeOH, steady-state and time-resolved fluorescence quenching of Py in MeOH by MV^{2+}, plot of kinetic traces at different wavelength of 20 mM MV^{2+} in MeOH, plot of kinetic traces at 600 nm (a) MV^{2+}, Py, and Py + 20 mM MV^{2+} in MeOH, plot of kinetic traces at different wavelength of Py + 10 mM MV^{2+} in MeOH, plot of kinetic traces at different wavelength of Py + 30 mM MV^{2+} in MeOH, plot of kinetic traces at different wavelength of Py + 40 mM MV^{2+} in MeOH, and plot of kinetic traces at different wavelength of Py + 20 mM MV^{2+} in EtOH. The Supporting Information is available free of charge on the ACS Publications website at DOI: 10.1021/acs.jpcb.5b03105.

■ AUTHOR INFORMATION

Corresponding Author

*E-mail: psen@iitk.ac.in.

Notes

The authors declare no competing financial interest.

■ ACKNOWLEDGMENTS

P.M. thanks UGC (University Grants Commission, Government of India) for awarding fellowships. We thank Prof. R. N. Mukherjee and Mr. Arunava Sengupta for helping in the cyclic voltammetry measurement. This work is financially supported by the Science and Engineering Research Board, Department of Science and Technology, Government of India (Project No. SR/S1/PC-08/2011), and IIT Kanpur.

■ REFERENCES

(1) Wang, H.; Lin, S.; Allen, J. P.; Williams, J. C.; Blankert, S.; Laser, C.; Woodbury, N. W. Protein Dynamics Control the Kinetics of Initial Electron Transfer in Photosynthesis. *Science* **2007**, *316*, 747−750.

(2) Whatley, F. R.; Tagawa, K.; Arnon, D. I. Separation of the Light and the Dark Reactions in Electron Transfer During Photosynthesis. *Proc. Natl. Acad. Sci. U. S. A.* **1963**, *49*, 266−270.

(3) Nishitani, S.; Kurata, N.; Sakata, Y.; Misumi, S. A New Model for the Study of Multistep Electron Transfer in Photosynthesis. *J. Am. Chem. Soc.* **1983**, *105*, 7771−7774.

(4) Fleming, G. R.; Martin, J. L.; Breton, J. Rates of Primary Electron Transfer in Photosynthetic Reaction Centers and Their Mechanistic Implications. *Nature* **1988**, *333*, 190−192.

(5) Martin, J. L.; Breton, J.; Hoff, A. J.; Migus, A.; Antonettl, A. Femtosecond Spectroscopy of Electron Transfer in the Reaction Center of the Photosynthetic Bacterium Rhodopseudomonas Sphaeroides R-26: Direct Electron Transfer from the Dimeric Bacteriochlorophyll Primary Donor to the Bacteriopheophytin Acceptor with a Time Constant of 2.8 ± 0.2 psec. *Proc. Natl. Acad. Sci. U. S. A.* **1986**, *83*, 957−961.

(6) Blazyk, J. L.; Gassner, G. T.; Lippard, S. J. Intermolecular Electron-Transfer Reactions in Soluble Methane Monooxygenase: A Role for Hysteresis in Protein Function. *J. Am. Chem. Soc.* **2005**, *127*, 17364−17376.

(7) Gray, H. B.; Winkler, J. R. Distant Charge Transport. *Proc. Natl. Acad. Sci. U. S. A.* **2005**, *102*, 3534−3539.

(8) Gray, H. B.; Winkler, J. R. Electron Tunneling Through Proteins. *Q. Rev. Biophys.* **2003**, *36*, 341−372.

(9) Bolton, J. R.; Mataga, N.; Mclendon, G. *Electron Transfer in Inorganic, Organic and Biological Systems*; Advances in Chemistry Series; American Chemical Society: Washington, DC, 1991; Vol. *228*.

(10) Photoinduced Electron Transfer. *Topics in Current Chemistry*; Matty, J., Ed.; Springer Verlag: Berlin, 1992; Vol. *163*.

(11) Chanton, M.; Fox, M. A. *Photoinduced Electron Transfer*; Elsevier: New York, 1988; Vol. *1−4*.

(12) Jortner, J.; Bixon, M. (Eds.), Electron Transfer from Isolated Molecules to Biomolecules, Advances in Chemical Physics parts 1 & 2, vols. *106 & 107*, Wiley, New York, 1999.

(13) Wasielewski, M. R. Photoinduced Electron Transfer in Supramolecular Systems for Artificial Photosynthesis. *Chem. Rev.* **1992**, *92*, 435−461.

(14) Karkas, M. D.; Johnston, E. V.; Akermark, B. Artificial Photosynthesis: from Nanosecond Electron Transfer to Catalytic Water Oxidation. *Acc. Chem. Res.* **2014**, *47*, 100−111.

(15) Noy, D.; Moser, C. C.; Dutton, P. L. Design and Engineering of Photosynthetic Light-Harvesting and Electron Transfer using Length, Time, and Energy Scales. *Biochim. Biophys. Acta, Bioenerg.* **2006**, *1757*, 90−105.

(16) Chan, W.; Tritsch, J. R.; Zhu, X. Y. Harvesting Singlet Fission for Solar Energy Conversion: One- versus Two-Electron Transfer from the Quantum Mechanical Superposition. *J. Am. Chem. Soc.* **2012**, *134*, 18295−18302.

(17) Krishnamurthy, S.; Kamat, P. V. CdSe−Graphene Oxide Light-Harvesting Assembly: Size Dependent Electron Transfer and Light Energy Conversion Aspects. *ChemPhysChem* **2014**, *15*, 2129−2135.

(18) Meyer, T. J. Chemical Approaches to Artificial Photosynthesis. *Acc. Chem. Res.* **1989**, *22*, 163−170.

(19) *Energy Resources through Photochemistry and Catalysis*; Gratzel, M., Ed.; Academic Press: New York, 1983.

(20) Grätzel, M. Dye-sensitized Solar Cells. *J. Photochem. Photobiol., C* **2003**, *4*, 145−153.

(21) Marcus, R. A. On the Theory of Oxidation-Reduction Reactions Involving Electron Transfer. I. *J. Chem. Phys.* **1956**, *24*, 966−978.

(22) Marcus, R. A. On the Theory of Oxidation-Reduction Reactions Involving Electron Transfer. II. Applications to Data on the Rates of Isotopic Exchange Reactions. *J. Chem. Phys.* **1957**, *26*, 867−871.

(23) Marcus, R. A. On the Theory of Oxidation-Reduction Reactions Involving Electron Transfer. III. Applications to Data on the Rates of Organic Redox Reactions. *J. Chem. Phys.* **1957**, *26*, 872−877.

(24) Marcus, R. A. Tutorial on Rate Constants and Reorganization Energies. *J. Electroanal. Chem.* **2000**, *483*, 2−6.

(25) Marcus, R. A. Exchange Reactions and Electron Transfer Reactions Including Isotopic Exchange. *Discuss. Faraday Soc.* **1960**, *29*, 21−31.

(26) Ghosh, S.; Sahu, K.; Mondal, S. K.; Sen, P.; Bhattacharyya, K. A Femtosecond Study of Photoinduced Electron Transfer from Dimethylaniline to Coumarin Dyes in a Cetyltrimethylammonium Bromide Micelle. *J. Chem. Phys.* **2006**, *125*, 054509−1−7.

(27) Rehm, D.; Weller, A. Kinetics of Fluorescence Quenching by Electron and H-atom Transfer. *Isr. J. Chem.* **1970**, *8*, 259−271.

(28) Bock, C. R.; Meyer, T. J.; Whitten, D. G. Photochemistry of Transition Metal Complexes. Mechanism and Efficiency of Energy Conversion by Electron-Transfer Quenching. *J. Am. Chem. Soc.* **1975**, *97*, 2909−2911.

(29) Nagle, J. K.; Dressick, W. J.; Meyer, T. J. Electron-Transfer Reactions in the "Abnormal" Free-energy Region. *J. Am. Chem. Soc.* **1979**, *101*, 3993−3995.

DOI: 10.1021/acs.jpcb.5b03105
J. Phys. Chem. B 2015, 119, 11253−11261

(30) Scheerer, R.; Graetzel, M. Laser Photolysis Studies of Duroquinone Triplet State Electron Transfer Reactions. *J. Am. Chem. Soc.* **1977**, *99*, 865−871.
(31) Eriksen, J.; Foote, C. S. Electron-Transfer Fluorescence Quenching and Exciplexes of Cyano-substituted Anthracenes. *J. Phys. Chem.* **1978**, *82*, 2659−2662.
(32) Ballardini, R.; Varani, G.; Indelli, M. T.; Scandola, F.; Balzani, V. Free Energy Correlation of Rate Constants for Electron Transfer Quenching of Excited Transition Metal Complexes. *J. Am. Chem. Soc.* **1978**, *100*, 7219−7223.
(33) Scandola, F.; Balzani, V. Free-energy Relationships for Electron-Transfer Processes. *J. Am. Chem. Soc.* **1979**, *101*, 6140−6142.
(34) Balzani, V.; Scandola, F.; Orlandi, G.; Sabbatini, N.; Indelli, M. T. The Nonadiabaticity Problem of Outer-Sphere Electron-Transfer Reactions. Reduction and Oxidation of Europium Ions. *J. Am. Chem. Soc.* **1981**, *103*, 3370−3378.
(35) Creutz, C.; Sutin, N. Vestiges of the "Inverted Region" for Highly Exergonic Electron-Transfer Reactions. *J. Am. Chem. Soc.* **1977**, *99*, 241−243.
(36) Miller, J. R.; Calcaterra, L. T.; Closs, G. L. Intramolecular Long-Distance Electron Transfer in Radical Anions. The Effects of Free Energy and Solvent on the Reaction Rates. *J. Am. Chem. Soc.* **1984**, *106*, 3047−3049.
(37) Kavarnos, G. J.; Turro, N. J. Photosensitization by Reversible Electron Transfer: Theories, Experimental Evidence, and Examples. *Chem. Rev.* **1986**, *86*, 401−449.
(38) Shirota, H.; Pal, H.; Tominaga, K.; Yoshihara, K. Substituent Effect and Deuterium Isotope Effect of Ultrafast Intermolecular Electron Transfer: Coumarin in Electron-Donating Solvent. *J. Phys. Chem. A* **1998**, *102*, 3089−3102.
(39) Pal, H.; Nagaswa, Y.; Tominaga, K.; Yoshihara, K. Deuterium Isotope Effect on Ultrafast Intermolecular Electron Transfer. *J. Phys. Chem.* **1996**, *100*, 11964−11974.
(40) Castner, E. W., Jr.; Kennedy, D.; Cave, R. J. Solvent as Electron Donor: Donor/Acceptor Electronic Coupling is a Dynamical Variable. *J. Phys. Chem. A* **2000**, *104*, 2869−2885.
(41) Nagasawa, Y.; Yartsev, A. P.; Tominaga, K.; Bisht, P. B.; Johnson, A. E.; Yoshihara, K. Dynamic Aspects of Ultrafast Intermolecular Electron Transfer Faster than Solvation Process: Substituent Effects and Energy Gap Dependence. *J. Phys. Chem.* **1995**, *99*, 653−662.
(42) Nad, S.; Pal, H. Electron Transfer from Aromatic Amines to Excited Coumarin Dyes: Fluorescence Quenching and Picosecond Transient Absorption Studies. *J. Phys. Chem. A* **2000**, *104*, 673−680.
(43) Ghosh, S.; Mondal, S. K.; Sahu, K.; Bhattacharyya, K. Ultrafast Photoinduced Electron Transfer from Dimethylaniline to Coumarin Dyes in Sodium Dodecyl Sulfate and Triton X-100 Micelles. *J. Chem. Phys.* **2007**, *126* (204708), 1−11.
(44) Ghosh, S.; Mondal, S. K.; Sahu, K.; Bhattacharyya, K. Ultrafast Electron Transfer in a Nanocavity. Dimethylaniline to Coumarin Dyes in Hydroxypropyl γ-Cyclodextrin. *J. Phys. Chem. A* **2006**, *110*, 13139−13144.
(45) Mandal, U.; Ghosh, S.; Dey, S.; Adhikari, A.; Bhattacharyya, K. Ultrafast Photoinduced Electron Transfer in the Micelle and the Gel Phase of a PEO-PPO-PEO Triblock Copolymer. *J. Chem. Phys.* **2008**, *128*, 164505.
(46) Kumbhakar, M.; Nath, S.; Mukherjee, T.; Pal, H. Intermolecular Electron Transfer between Coumarin Dyes and Aromatic Amines in Triton-X-100 Micellar Solutions: Evidence for Marcus Inverted Region. *J. Chem. Phys.* **2004**, *120*, 2824−2834.
(47) Kumbhakar, M.; Singh, P. K.; Satpati, S. K.; Nath, S.; Pal, H. Ultrafast Electron Transfer Dynamics in Micellar Media using Surfactant as the Intrinsic Electron Acceptor. *J. Phys. Chem. B* **2010**, *114*, 10057−10065.
(48) Satpati, S. K.; Kumbhakar, M.; Nath, S.; Pal, H. Photoinduced Electron Transfer between Quinones and Amines in Micellar Media: Tuning the Marcus Inversion Region. *J. Photochem. Photobiol., A* **2008**, *200*, 270−276.
(49) Kumbhakar, M.; Singh, P. K.; Nath, S.; Bhasikuttan, A. C.; Pal, H. Ultrafast Bimolecular Electron Transfer Dynamics in Micellar Media. *J. Phys. Chem. B* **2008**, *112*, 6646−6652.
(50) Bhattacharyya, K. Solvation Dynamics and Proton Transfer in Supramolecular Assemblies. *Acc. Chem. Res.* **2003**, *36*, 95−101.
(51) Bhattacharyya, K.; Bagchi, B. Slow Dynamics of Constrained Water in Complex Geometries. *J. Phys. Chem. A* **2000**, *104*, 10603−10613.
(52) Nandi, N.; Bhattacharyya, K.; Bagchi, B. Dielectric Relaxation and Solvation Dynamics of Water in Complex Chemical and Biological Systems. *Chem. Rev.* **2000**, *100*, 2013−2046.
(53) Riter, R. E.; Willard, D. M.; Levinger, N. E. Water Immobilization at Surfactant Interfaces in Reverse Micelles. *J. Phys. Chem. B* **1998**, *102*, 2705−2714.
(54) Piletic, I. R.; Moilanen, D. E.; Spry, D. B.; Levinger, N. E.; Fayer, M. D. Testing the Core/Shell Model of Nanoconfined Water in Reverse Micelles using Linear and Nonlinear IR Spectroscopy. *J. Phys. Chem. A* **2006**, *110*, 4985−4999.
(55) Senapati, S.; Chandra, A. Dielectric Constant of Water Confined in a Nanocavity. *J. Phys. Chem. B* **2001**, *105*, 5106−5109.
(56) Paul, A.; Samanta, A. Photoinduced Electron Transfer Reaction in Room Temperature Ionic Liquids: A Combined Laser Flash Photolysis and Fluorescence Study. *J. Phys. Chem. B* **2007**, *111*, 1957−1962.
(57) Santhosh, K.; Samanta, A. Modulation of the Excited State Intramolecular Electron Transfer Reaction and Dual Fluorescence of Crystal Violet Lactone in Room Temperature Ionic Liquids. *J. Phys. Chem. B* **2010**, *114*, 9195−9200.
(58) Marcus, R. A.; Sutin, N. Electron Transfer in Chemistry and Biology. *Biochim. Biophys. Acta, Rev. Bioenerg.* **1985**, *811*, 265−322.
(59) Rosspeintner, A.; Koch, M.; Angulo, G.; Vauthey, E. Spurious Observation of the Marcus Inverted Region in Bimolecular Photo-induced Electron Transfer. *J. Am. Chem. Soc.* **2012**, *134*, 11396−11399.
(60) Koch, M.; Rosspeintner, A.; Angulo, G.; Vauthey, E. Bimolecular Photoinduced Electron Transfer in Imidazolium based Room Temperature Ionic Liquids is not faster than Conventional Solvents. *J. Am. Chem. Soc.* **2012**, *134*, 3729−3736.
(61) Rosspeintner, A.; Vauthey, E. Bimolecular Photoinduced Electron Transfer Reactions in Liquids under the Gaze of Ultrafast Spectroscopy. *Phys. Chem. Chem. Phys.* **2014**, *16*, 25741−25754.
(62) Navalon, S.; de Miguel, M.; Martin, R.; Alvaro, M.; Garcia, H. Enhancement of the Catalytic Activity of Supported Gold Nanoparticles for the Fenton Reaction by Light. *J. Am. Chem. Soc.* **2011**, *133*, 2218−2226.
(63) Hayashi, T.; Takimura, T.; Ogoshi, H. Photoinduced Singlet Electron Transfer in a Complex Formed from Zinc Myoglobin and Methyl Viologen: Artificial Recognition by a Chemically Modified Porphyrin. *J. Am. Chem. Soc.* **1995**, *117*, 11606−11607.
(64) Nakato, T.; Watanabe, S.; Kamijo, Y.; Nono, Y. Photoinduced Electron Transfer between Ruthenium-bipyridyl Complex and Methylviologen in Suspensions of Smectite Clays. *J. Phys. Chem. C* **2012**, *116*, 8562−8570.
(65) Chaudhuri, M. K.; Ghosh, S. K. Novel Synthesis of Tris(acetylacetonato)iron(III). *J. Chem. Soc., Dalton Trans.* **1983**, 839−840.
(66) Snellenburg, J. J.; Laptenok, S. P.; Seger, R.; Mullen, K. M.; vanStokkum, I. H. M. Glotaran: A Java Based Graphical User Interface for the R Package TIMP. *J. Stat. Softw.* **2012**, *49* (3), 1−22.
(67) Watanabe, T.; Honda, K. Measurement of the Extinction Coefficient of the Methyl Viologen Cation Radical and the Efficiency of its Formation by Semiconductor Photocatalysis. *J. Phys. Chem.* **1982**, *86*, 2617−2619.
(68) Miyasaka, H.; Masuhara, H.; Mataga, N. Picosecond Absorption Spectra and Relaxation Processed of the Excited Singlet State of Pyrene in Solution. *Laser Chem.* **1983**, *1*, 357−386.
(69) Foggi, P.; Pettini, L.; Santa, I.; Righini, R.; Califano, S. Transient Absorption and Vibrational Relaxation Dynamics of the Lowest Excited Singlet State of Pyrene in Solution. *J. Phys. Chem.* **1995**, *99*, 7439−7445.

DOI: 10.1021/acs.jpcb.5b03105
J. Phys. Chem. B 2015, 119, 11253−11261

(70) Peon, J.; Tan, X.; Hoerner, J. D.; Xia, C.; Luk, Y. F.; Kohler, B. Excited State Dynamics of Methyl Viologen. Ultrafast Photoreduction in Methanol and Fluorescence in Acetonitrile. *J. Phys. Chem. A* **2001**, *105*, 5768−5777.

DOI: 10.1021/acs.jpcb.5b03105
J. Phys. Chem. B 2015, 119, 11253−11261